# Correlations and Semi-Universal Relations Connecting Nuclear Matter and Neutron Stars

J. M. Lattimer

Department of Physics & Astronomy


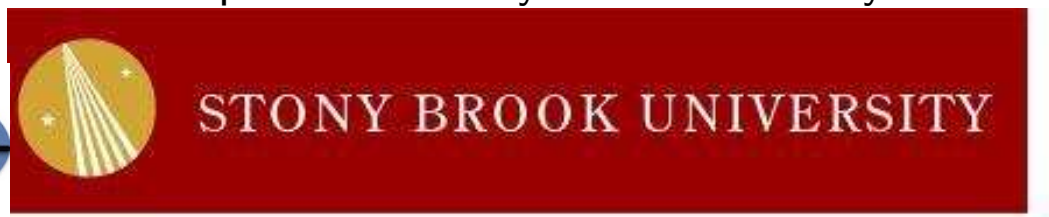



Neutrino Frontiers
Galileo Galilei Institute for Theoretical Physics

Arcetri, Florence, Italy
11 July, 2024

# Acknowledgements

**Funding Support:**

DOE - Nuclear Physics

DOE - Toward Exascale Astrophysics of Mergers and Supernovae (TEAMS)

NASA - Neutron Star Interior Composition ExploreR (NICER)

NSF - Neutrinos, Nuclear Astrophysics and Symmetries (PFC - N3AS)

DOE - Nuclear Physics from Multi-Messenger Mergers (NP3M)

**Recent Collaborators:**

Boyang Sun (Stony Brook), Duncan Brown & Soumi De (Syracuse), Christian Drischler, Madappa Prakash & Tianqi Zhao (Ohio), Sophia Han (TDLI), Sanjay Reddy (INT), Achim Schwenk (Darmstadt), Andrew Steiner (Tennessee) & Ingo Tews (LANL)

# Neutron Stars: Basics

- Nearly all known NSs are pulsars (rapidly rotating and highly magnetized) that emit X-ray, optical or radio beams from their poles, like a lighthouse.

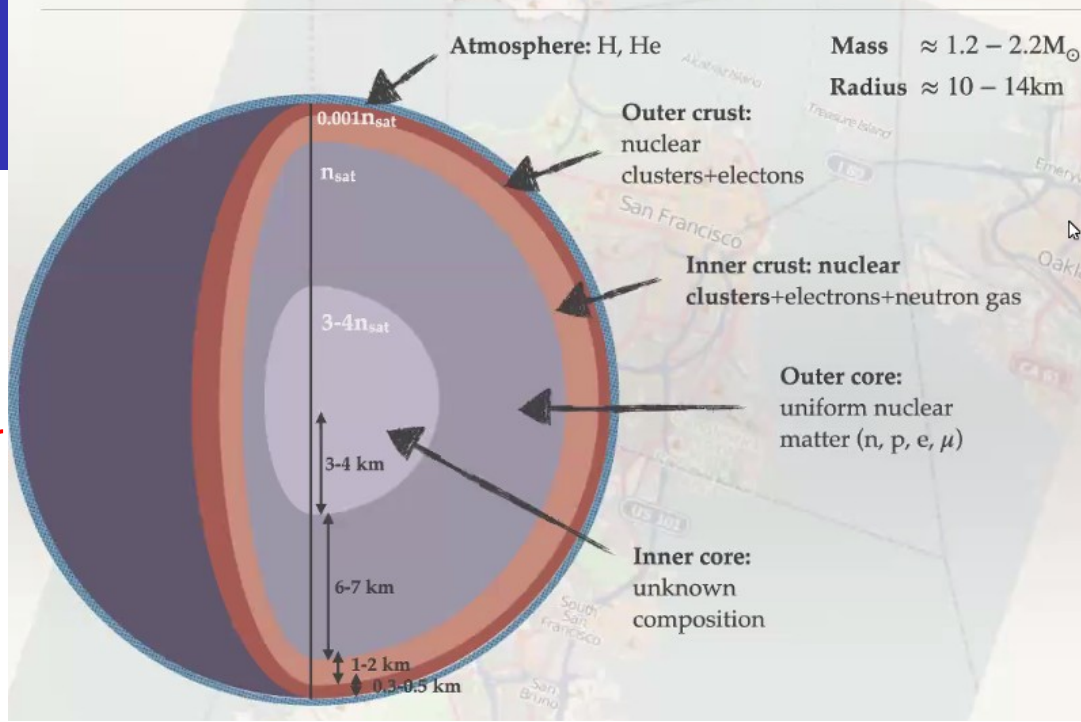


- The radii of most NSs are about 12 km.
- Most, if not all, NSs are formed in the gravitational collapse of massive stars at the ends of their lives; some of those collapses produce black holes instead. Some massive NSs may be formed in the aftermath of a binary merger of two lower-massed neutron stars.
- The minimum possible NS mass is $0.1M_\odot$, but none are observed to be less massive than $1M_\odot$.

# Pulsar Timing for PSR J0737-3039

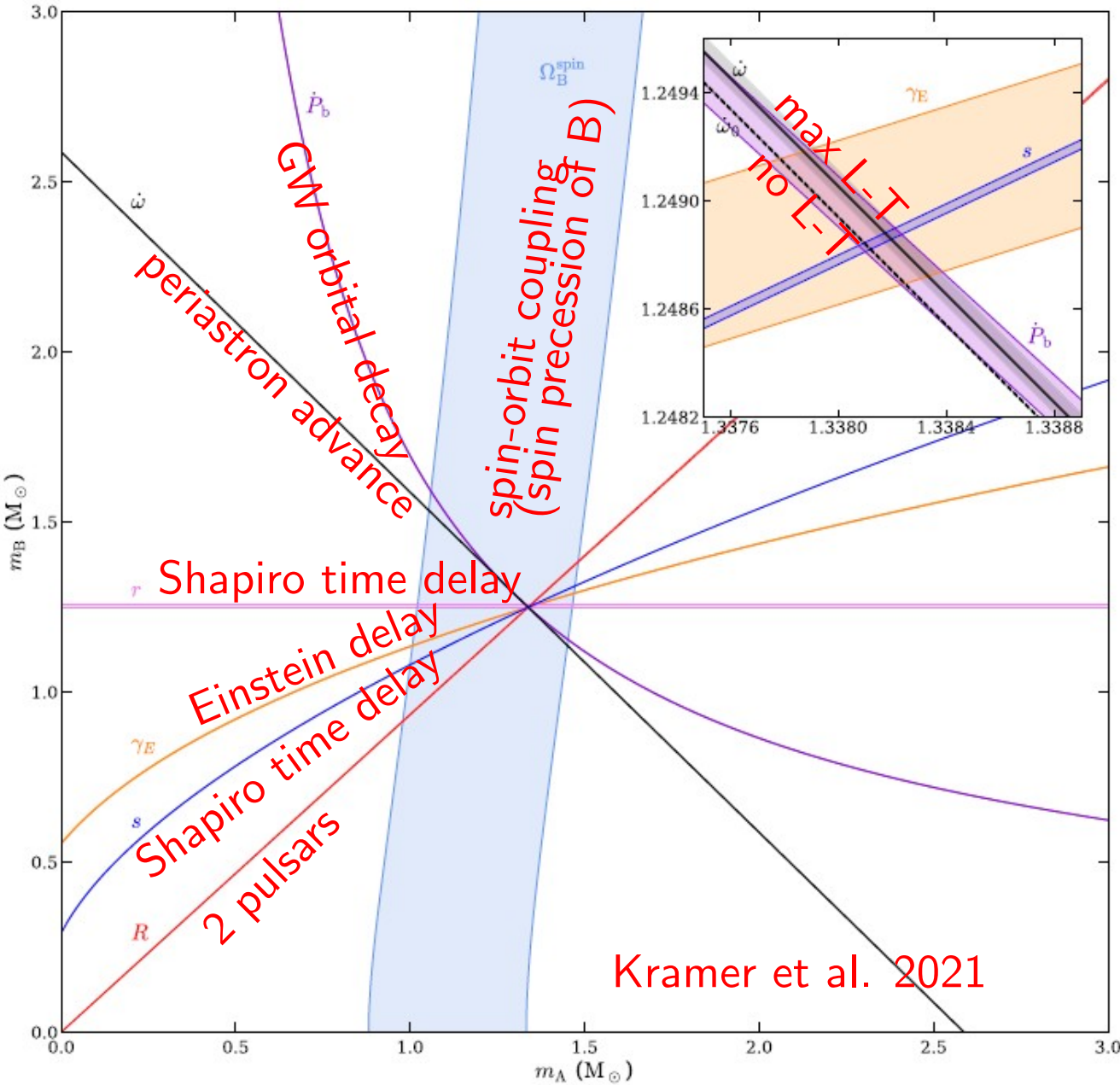


$m_A = 1.338185^{+12}_{-14}\ M_\odot$

$m_B = 1.248868^{+13}_{-11}\ M_\odot$

These are the most precisely known masses of any astronomical objects.

# Masses of Pulsars in Binaries from Pulsar Timing

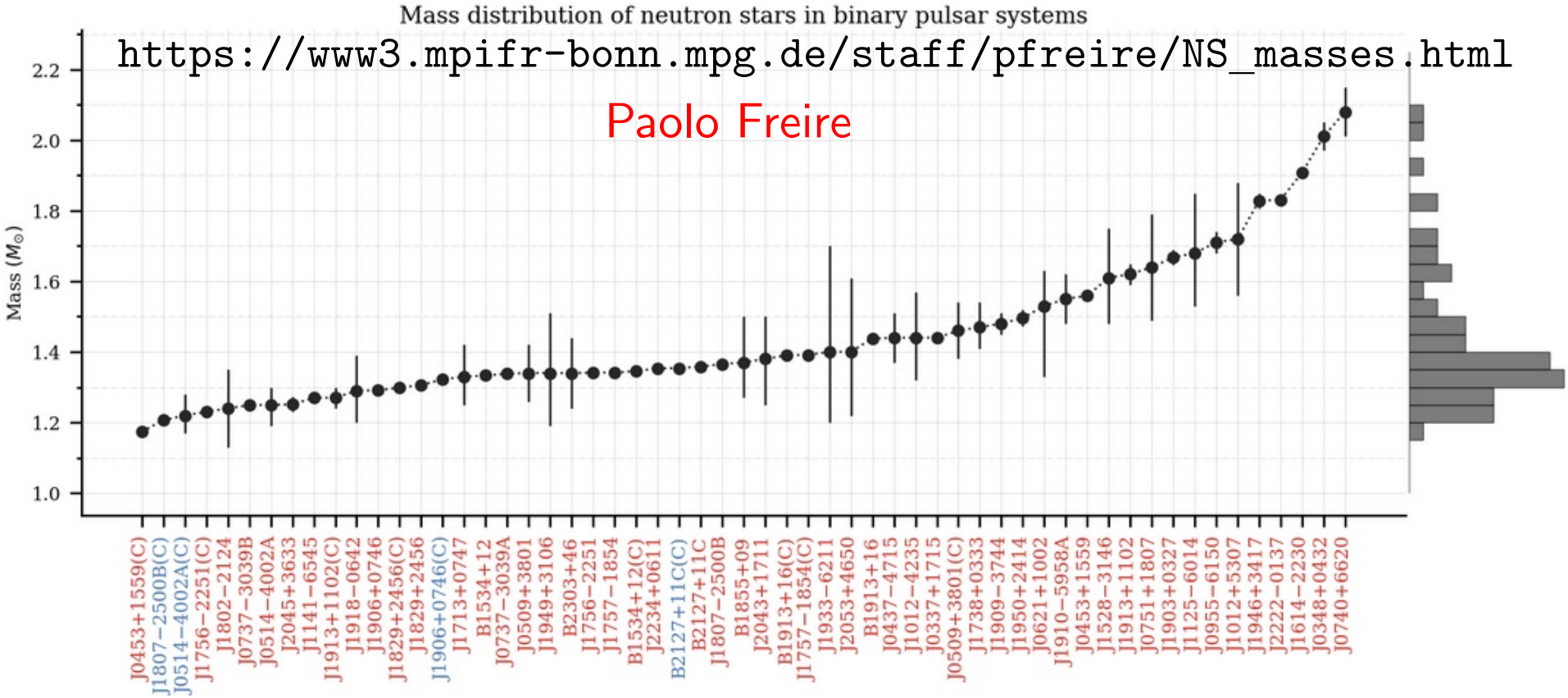


Largest: $2.08 \pm 0.07$ $M_\odot$
Smallest: $1.174 \pm 0.004$ $M_\odot$

Several other NS masses have been measured by other means, including some estimated to be more than $2M_\odot$ (e.g., black widow pulsars) and smaller than $1M_\odot$ (HESS J1731-347), but their mass uncertainties are generally large.

# How Can a Neutron Star's Radius Be Measured?

- Flux $= \frac{\text{Luminosity}}{4\pi D^2} = \frac{4\pi R^2 \sigma_B T_s^4}{4\pi D^2} = \left(\frac{R}{D}\right)^2 \sigma_B T_s^4$
  X-ray observations of quiescent neutron stars in low-mass X-ray binaries measure the flux and surface temperature $T_s$. Distance $D$ somewhat uncertain; GR effects introduce an $M$ dependence.
- $F_{Edd} = \frac{GMc}{\kappa D^2}$ X-ray observations of bursting neutron stars in accreting systems measure the Eddington flux $F_{Edd}$. $\kappa$ is the poorly-known opacity; GR effects introduce an $R$ dependence.
- X-ray phase-resolved spectroscopy of millisecond pulsars with nonuniform surface emissions (hot spots). NICER: PSR J0030+0451, PSR J0437-4715 (closest and brightest millisecond pulsar) and PSR J0740+6620 (most massive pulsar).
- $R_{1.4} \simeq (11.5 \pm 0.3) \frac{\mathcal{M}}{M_\odot} \left(\frac{\tilde{\Lambda}}{800}\right)^{1/6}$ km, $\quad \mathcal{M} = \frac{(M_A M_B)^{3/5}}{(M_A + M_B)^{1/5}}$
  GW observations of neutron star mergers measure the chirp mass $\mathcal{M}$ and binary tidal deformability $\tilde{\Lambda}$ (GW170817).
- $I_A \propto M_A R_A^2$ Radio observations of extremely relativistic binary pulsars measure masses $M_A, M_B$ and moment of inertia $I_A$ from spin-orbit coupling [PSR J0737-3039 ($P_b = 0.102$d), PSR J1757-1854 (0.164 d), PSR J1946+2052 (0.078 d)].

# Summary of Astrophysical Observations

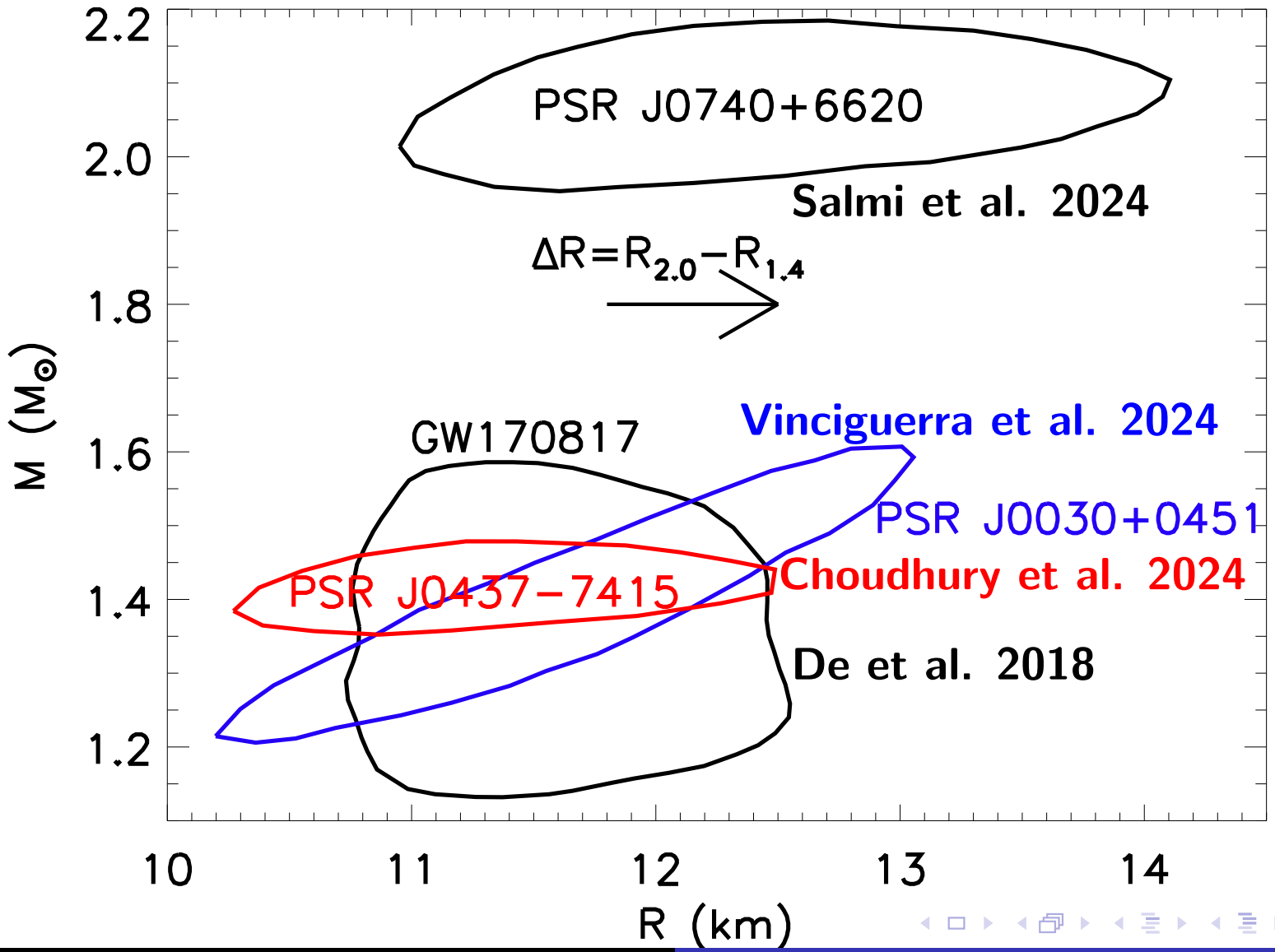

# Neutron Star Structure

## Tolman-Oppenheimer-Volkov equations

$$\frac{dp}{dr} = -\frac{G}{c^4}\frac{(mc^2 + 4\pi pr^3)(\varepsilon + p)}{r(r - 2Gm/c^2)}$$

$$\frac{dm}{dr} = 4\pi\frac{\varepsilon}{c^2}r^2$$

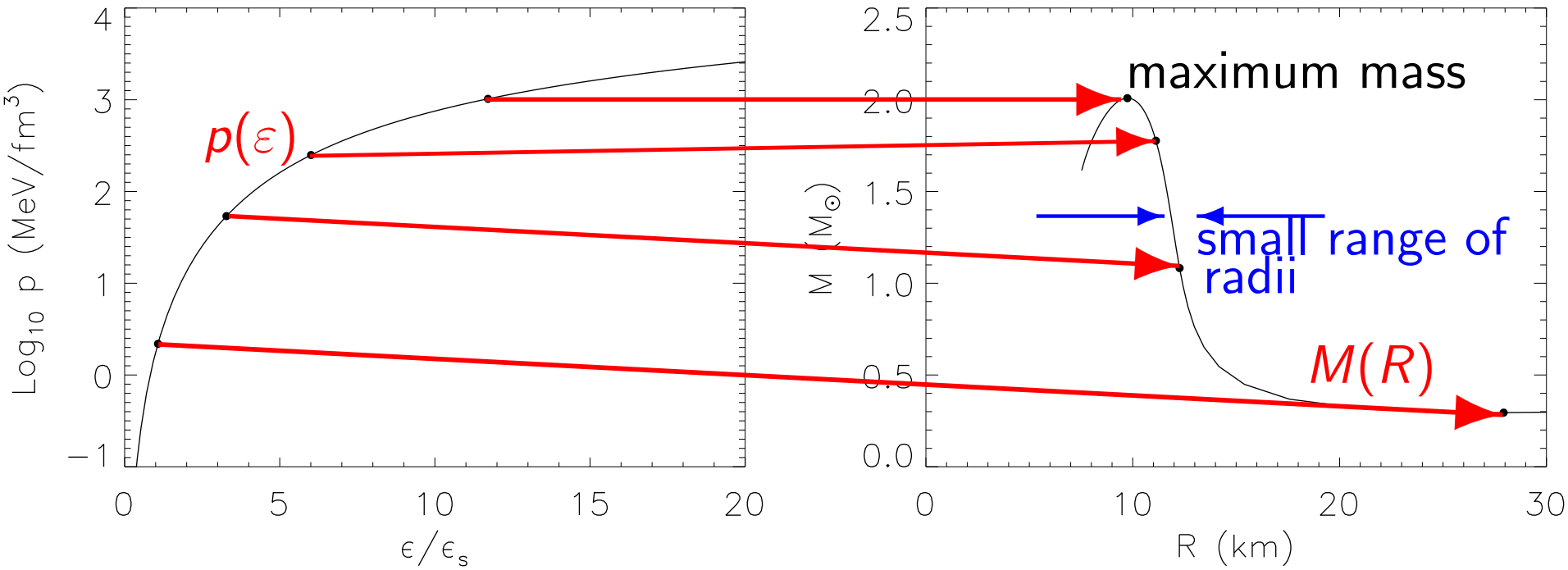


Equation of State ⟵ Observations

# The Radius – Pressure Correlation

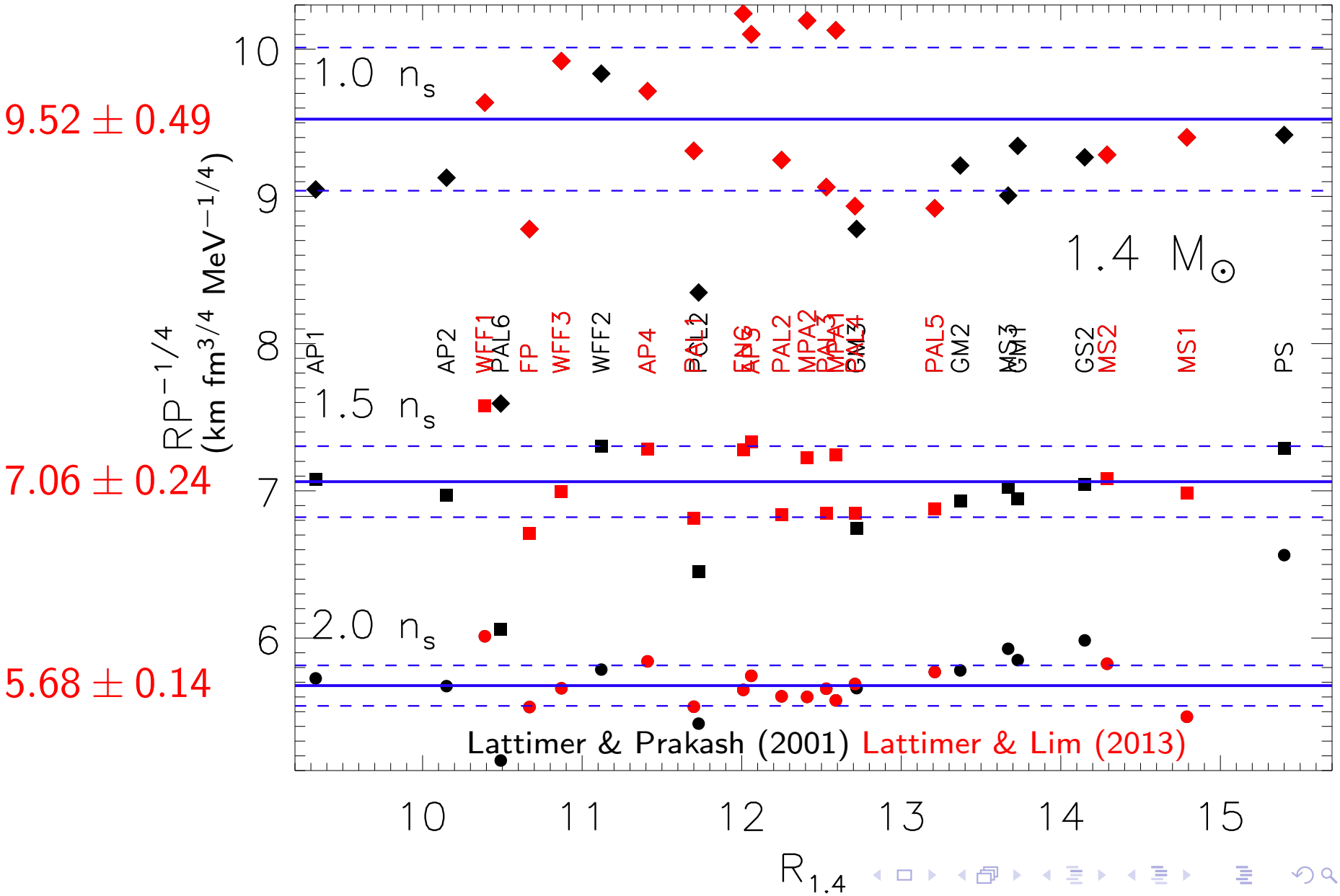

# The I-Love Relation

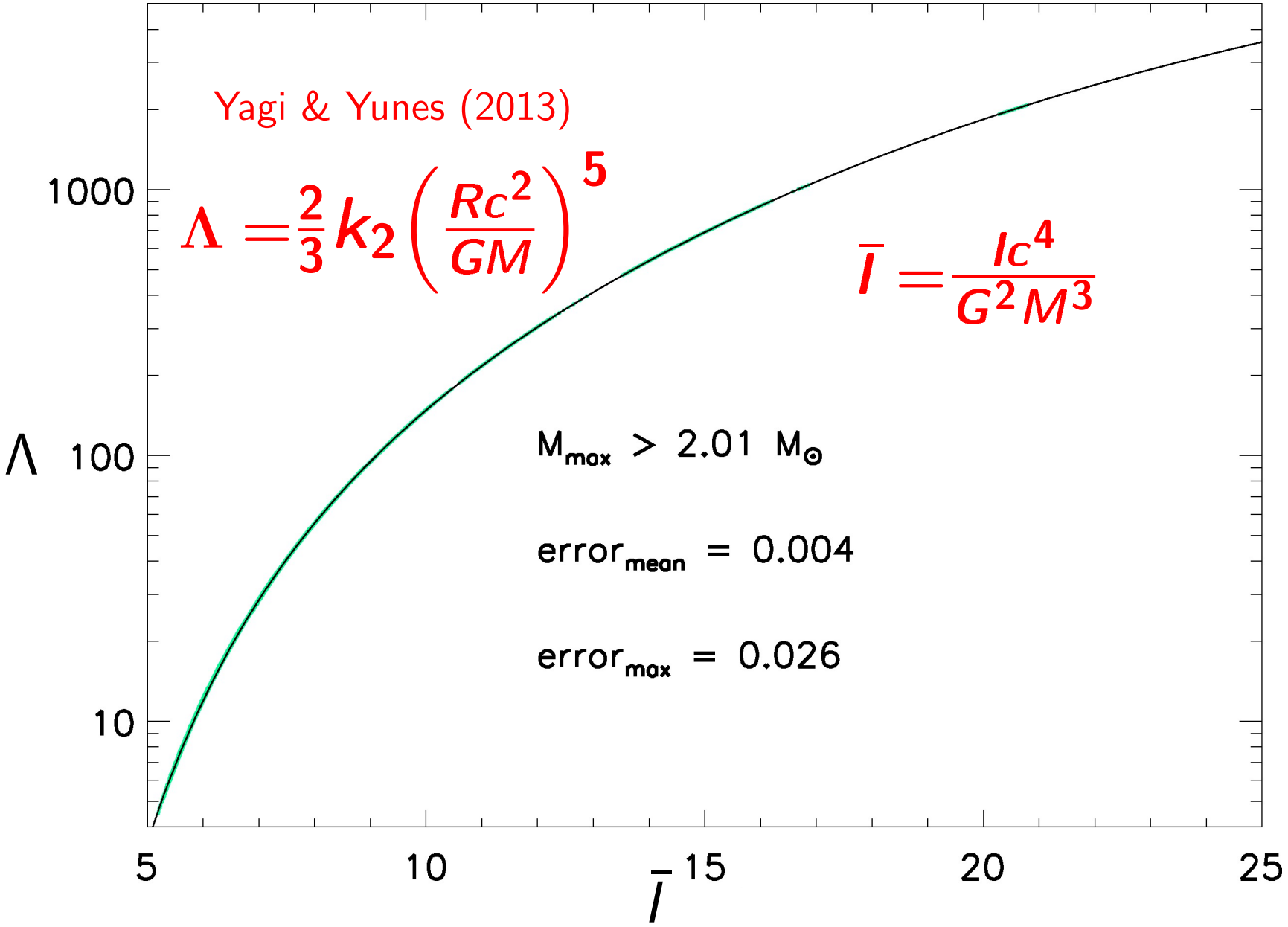

# F-Mode Properties - Moment of Inertia

$$\Omega_f = \frac{GM\omega_f}{c^3}$$

Zhao & Lattimer 2022

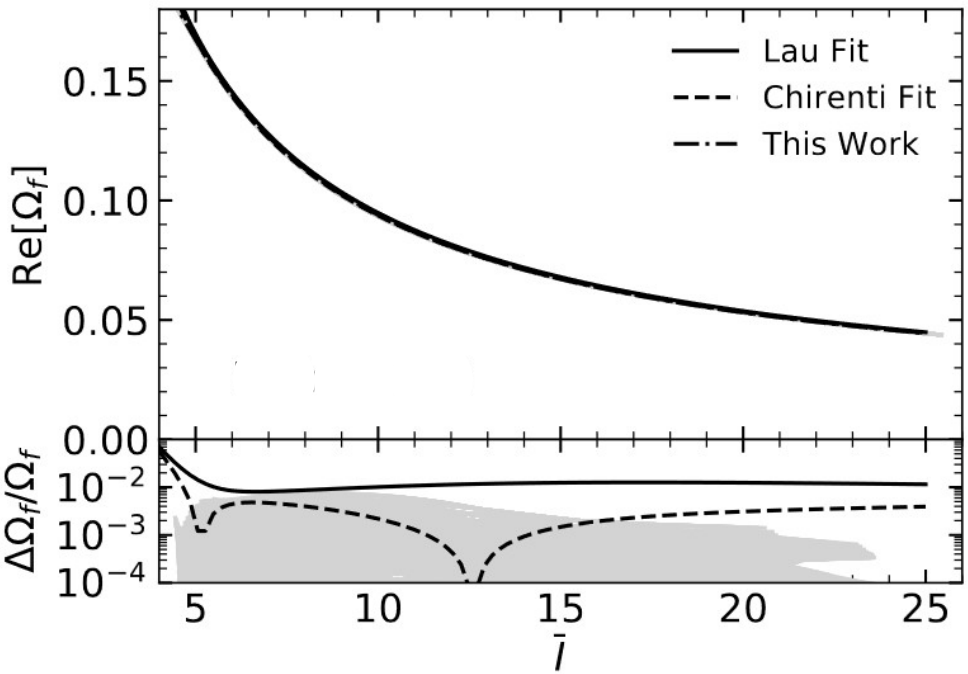


frequency

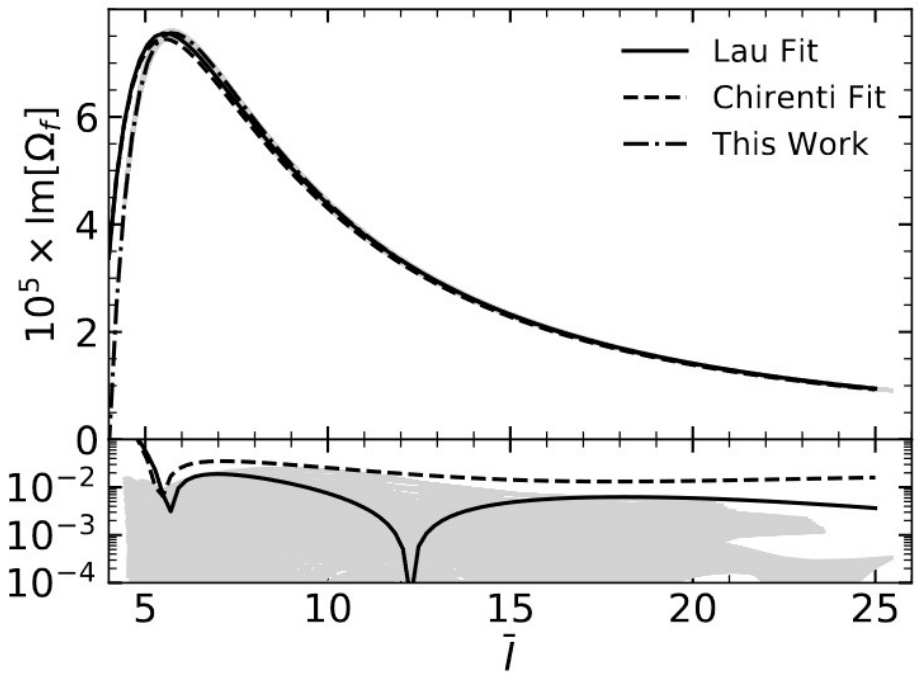


damping time

# Neutron Skin Thickness - $L$

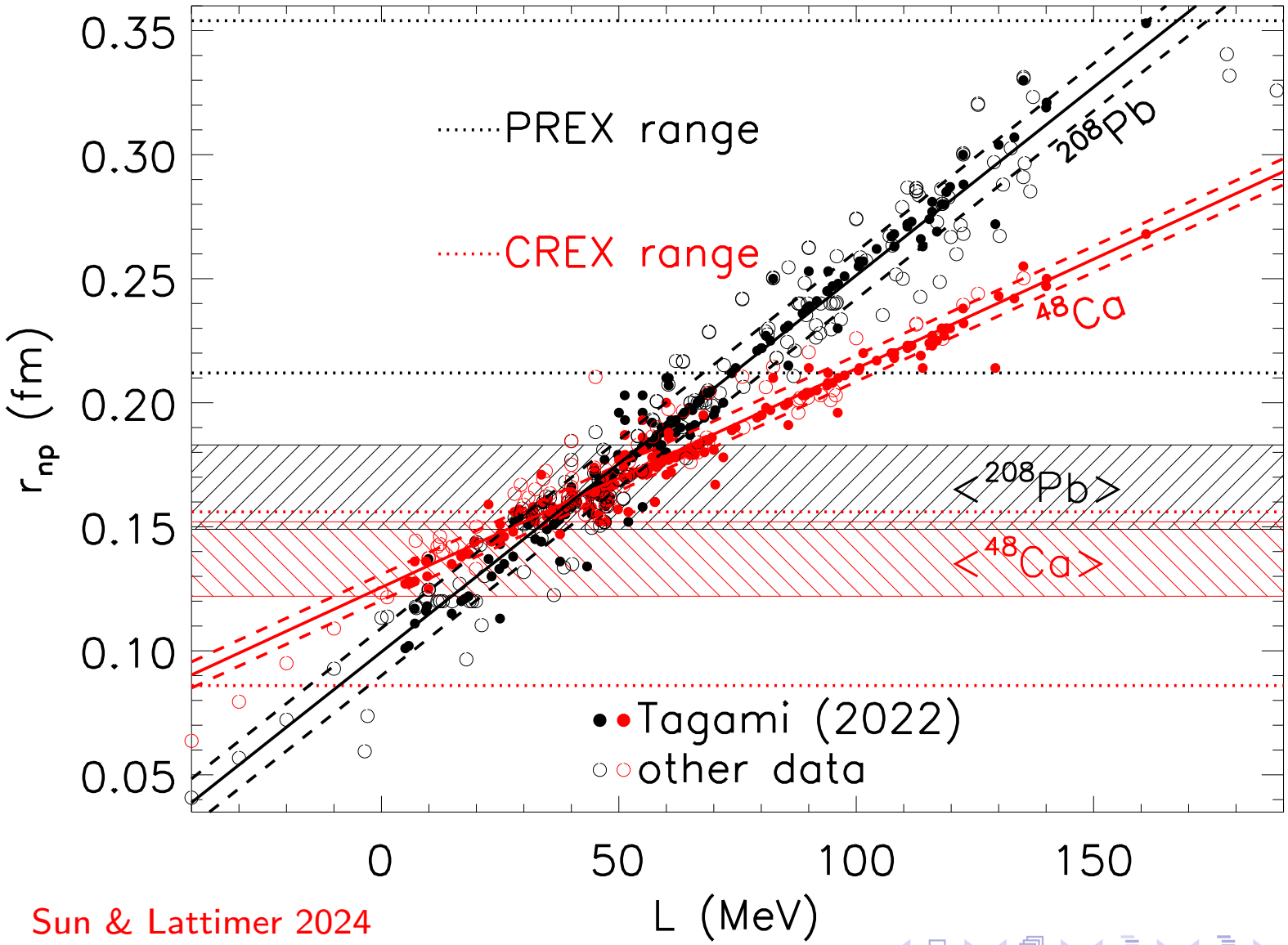


Sun & Lattimer 2024

# Maximum Mass As a Unique Scaling Point

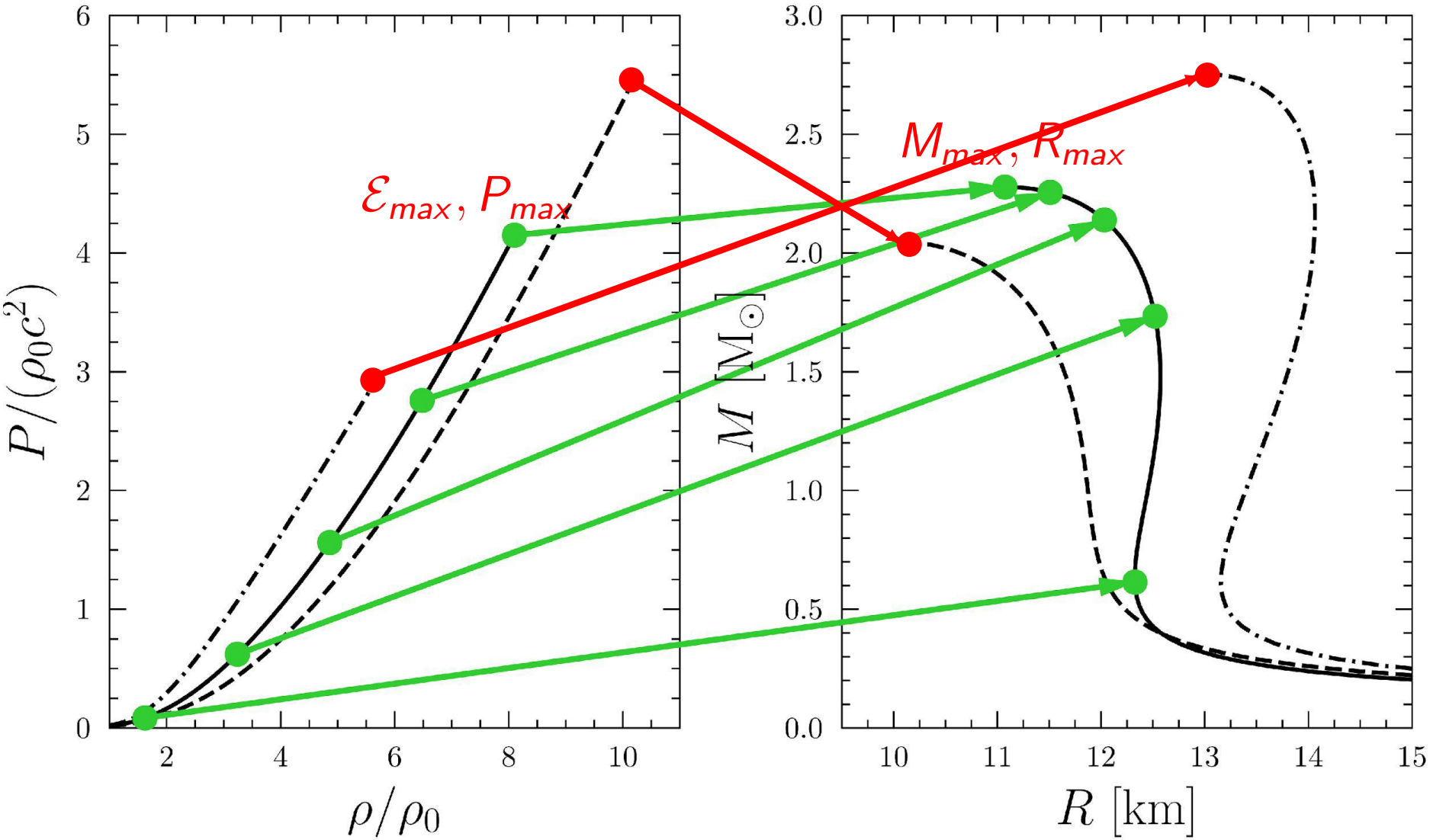

# Varying the EOS

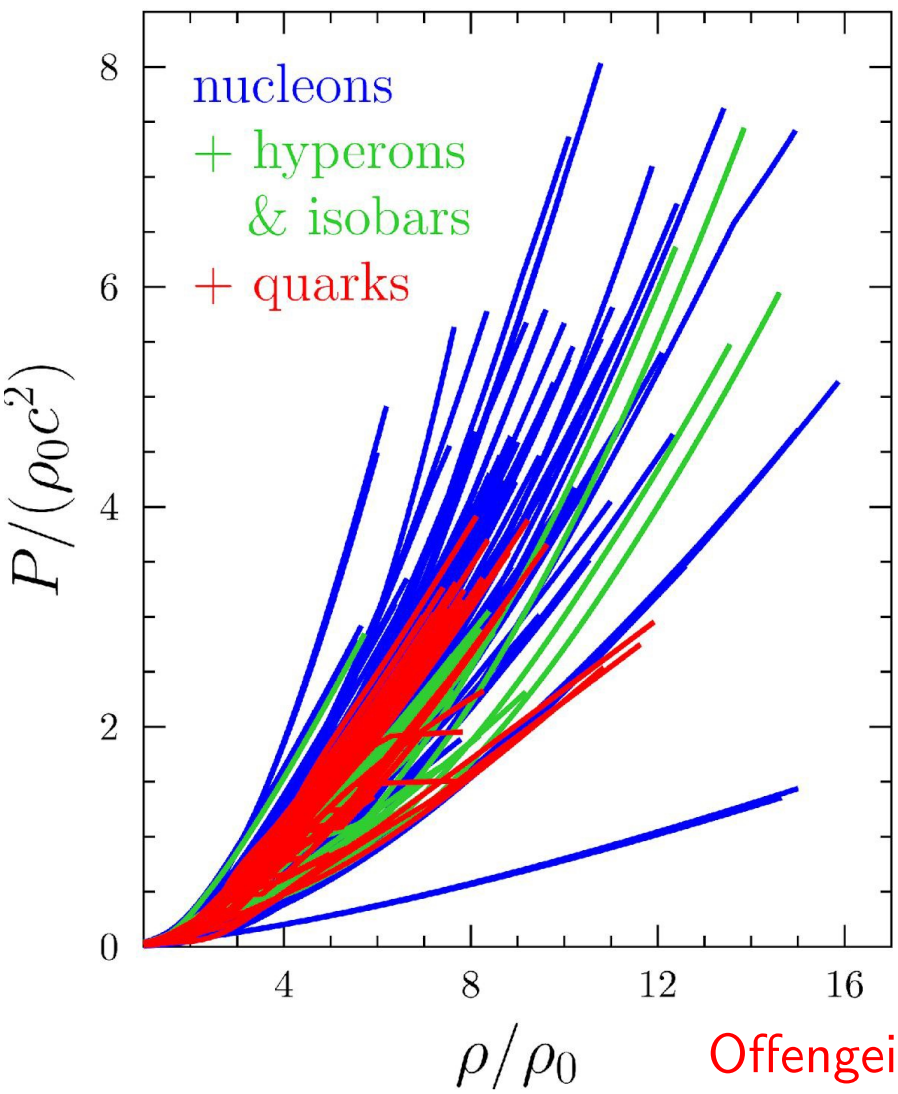


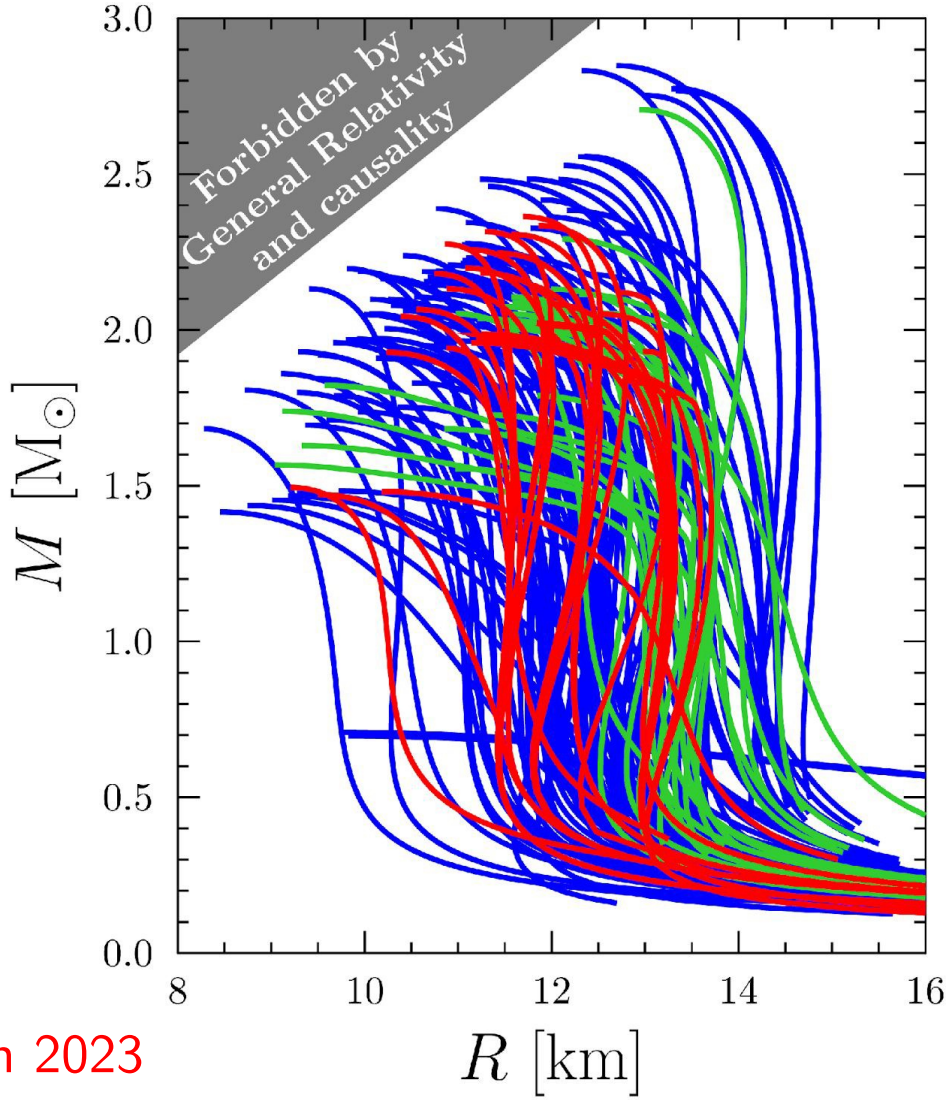


Offengeim 2023

# $M_{\rm max}, R_{\rm max}, \mathcal{E}_{\rm max}, P_{\rm max}$ Correlations

- Ofengeim(2020) fitted $\mathcal{E}_{max}$ and $P_{max}$ with the functions

$$\mathcal{E}_{max}, P_{max} \simeq \left[ \frac{a_{\mathcal{E},P}}{R_{max} \cos\phi_{\mathcal{E},P} + (GM_{max}/c^2) \sin\phi_{\mathcal{E},P} + d_{\mathcal{E},P}} \right]^{s_{\mathcal{E},P}}$$

with accuracies of about 3% and 8%, respectively.

- Cai, Li and Zhang (2023) found a perturbative solution of the TOV equations in the parameter $x = P_c/\mathcal{E}_c$:

$$R \simeq \sqrt{\frac{3c^2}{2\pi G \mathcal{E}_c}} \left[ \frac{x}{1+4x+3x^2} \right]^{1/2},$$

$$M \simeq \sqrt{\frac{54c^6}{\pi G^3 \mathcal{E}_c}} \left[ \frac{x}{1+4x+3x^2} \right]^{3/2}.$$

At $M_{max}$, accuracies are 7% and 8%; at $1.4M_\odot$, they are 2% and 6%.

- Ofengeim et al. (2023) suggested fits for $M_{max}, R_{max}$:

$$M_{max} \simeq \frac{a_M \mathcal{E}_{max}^{-1/2} x^{3/2}}{b_M + c_M x^{p_M} \mathcal{E}_{max}^{q_M}}, \qquad R_{max} \simeq \frac{a_R \mathcal{E}_{max}^{-1/2} x^{1/2}}{b_R + c_R x^{p_R} \mathcal{E}_{max}^{q_R}}$$

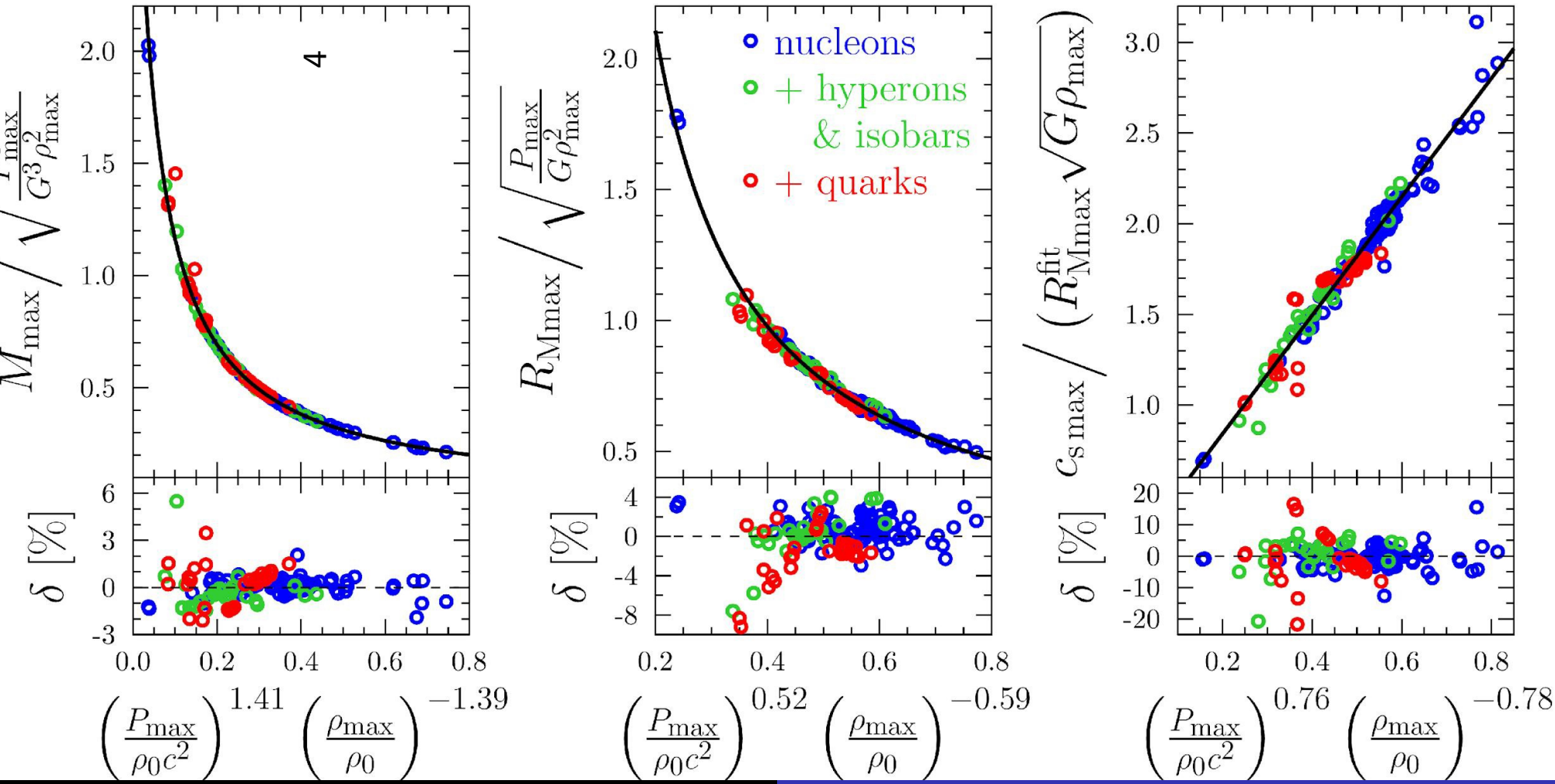

# $M_{\rm max}, R_{\rm max}, \mathcal{E}_{\rm max}, P_{\rm max}$ Correlation

Ofengeim et al's finding suggest the power-law correlations

$$\mathcal{E}_{\rm c,max} = (1.809 \pm 0.36) \left(\frac{R_{\rm max}}{10{\rm km}}\right)^{-1.98} \left(\frac{M_{\rm max}}{M_\odot}\right)^{-0.171} \ {\rm GeV\ fm^{-3}},$$

$$P_{\rm c,max} = (118.5 \pm 6.2) \left(\frac{R_{\rm max}}{10{\rm km}}\right)^{-5.24} \left(\frac{M_{\rm max}}{M_\odot}\right)^{2.73} \ {\rm MeV\ fm^{-3}},$$

which are accurate to about 5% in fitting $\mathcal{E}_{c,max}$ and $P_{c,max}$.

Points along $M - R$ curves, at $M = fM_{\rm max}$, have similarly accurate correlations:

$$\mathcal{E}_{c,f} = a_{\mathcal{E},f} R_{fM_{max}}^{b_{\mathcal{E},f}} M_{max}^{c_{\mathcal{E},f}}$$

$$P_{c,f} = a_{P,f} R_{fM_{max}}^{b_{P,f}} M_{max}^{c_{P,f}}$$

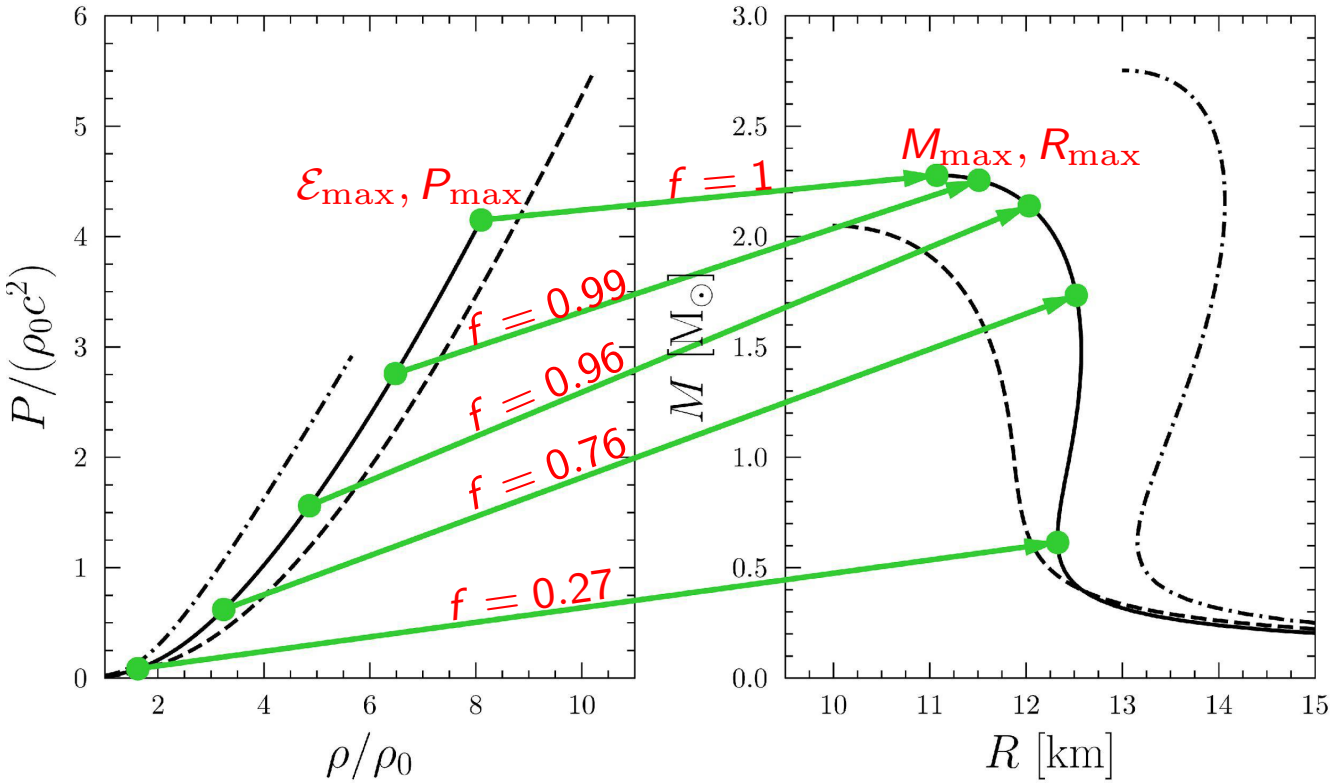

# $(M, R)$ Is Not Equivalent To $(\mathcal{E}_c, P_c)$

While the maximum mass point $(M_{max}, R_{max})$ predicts $(\mathcal{E}_{c,max}, P_{c,max})$ to about 5%, and similarly for a given fractional maximum mass $fM_{max}$, the inversion is not unique. Two different equations of state predicting the same $(M, R)$ (numbers in figure) arrive at those values from integration via different paths in $(\mathcal{E}, P)$ space. Similarly, two equations of state with identical values of $(\mathcal{E}_c, P_c)$ (letters) do not have the same $(M, R)$ values.

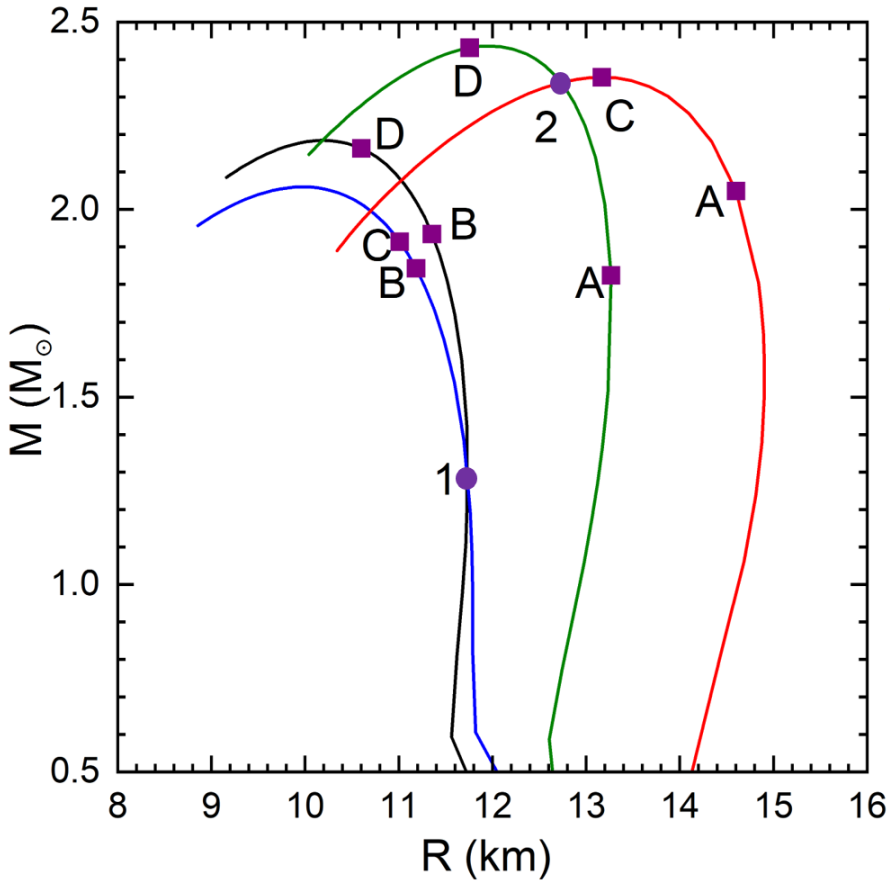


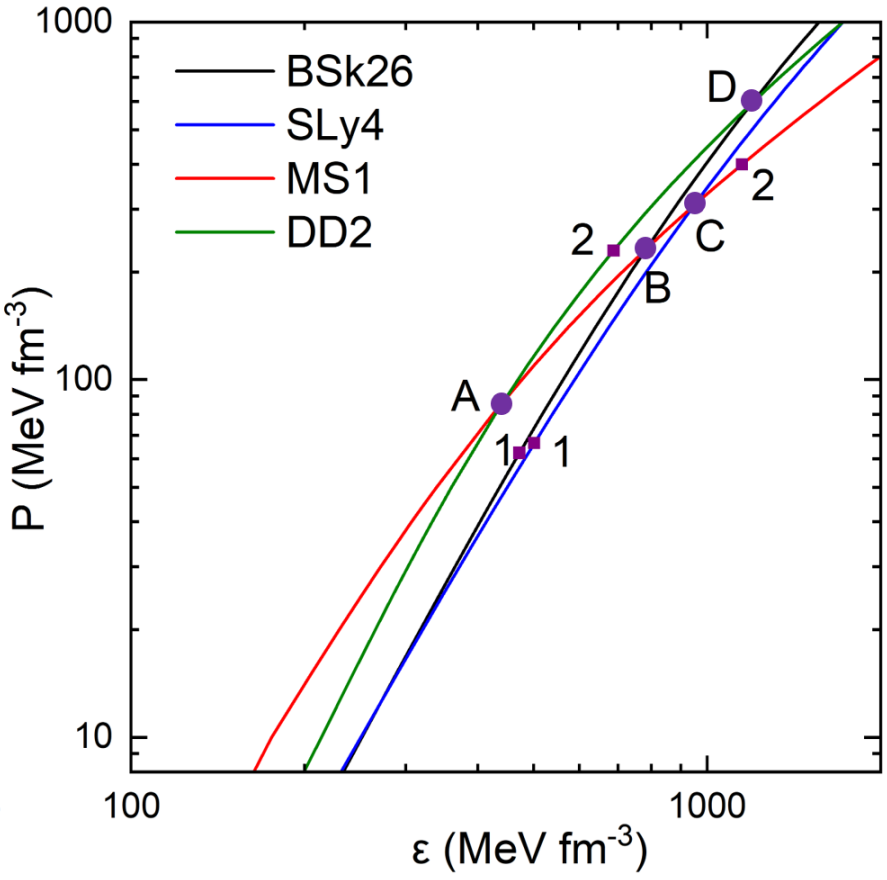

# Correlations at $M = fM_{\rm max}$

Thus, more information than $(M, R)$ needed. We find precision is greatly improved using a 2nd radius from a grid of fractional $M_{max}$ points, *e.g.*, $f \in [1, 0.95, 0.9, 0.85, 4/5, 3/4, 2/3, 0.6, 0.5, 0.4, 1/3]$.

$$\mathcal{E}_f = a_{\mathcal{E},f} \left(\frac{R_{f_1}}{10\rm km}\right)^{b_{\mathcal{E},f_1}} \left(\frac{R_{f_2}}{10\rm km}\right)^{c_{\mathcal{E},f_2}} \left(\frac{M_{max}}{M_\odot}\right)^{d_{\mathcal{E},f}},$$

$$P_f = a_{P,f} \left(\frac{R_{f_1}}{10\rm km}\right)^{b_{P,f_1}} \left(\frac{R_{f_2}}{10\rm km}\right)^{c_{P,f_2}} \left(\frac{M_{max}}{M_\odot}\right)^{d_{P,f}},$$

| $f = M/M_{\rm max}$ | $f_1$ | $f_2$ | $\Delta(\ln \mathcal{E}_f)$ | $f_1$ | $f_2$ | $\Delta(\ln P_f)$ |
|---|---|---|---|---|---|---|
| 1 | 0.95 | 0.9 | 0.00469 | 1 | 3/5 | 0.0123 |
| 0.95 | 0.95 | 4/5 | 0.00275 | 0.95 | 3/5 | 0.00722 |
| 0.90 | 0.95 | 2/3 | 0.00227 | 0.95 | 0.4 | 0.00517 |
| 0.85 | 0.95 | 1/2 | 0.00237 | 0.9 | 0.4 | 0.00491 |
| 4/5 | 0.9 | 1/2 | 0.00230 | 0.85 | 0.4 | 0.00463 |
| 3/4 | 0.85 | 1/2 | 0.00239 | 0.8 | 0.4 | 0.00539 |
| 2/3 | 3/4 | 1/2 | 0.00277 | 2/3 | 0.4 | 0.00513 |
| 3/5 | 3/4 | 0.4 | 0.00339 | 2/3 | 1/3 | 0.0172 |
| 1/2 | 2/3 | 1/3 | 0.00477 | 1/2 | 0.4 | 0.00996 |
| 2/5 | 1/2 | 1/3 | 0.00706 | 1/2 | 1/3 | 0.0187 |
| 1/3 | 1/2 | 1/3 | 0.0122 | 2/5 | 1/3 | 0.0259 |

**greatly reduced uncertaintites!**

# Testing the Inversion

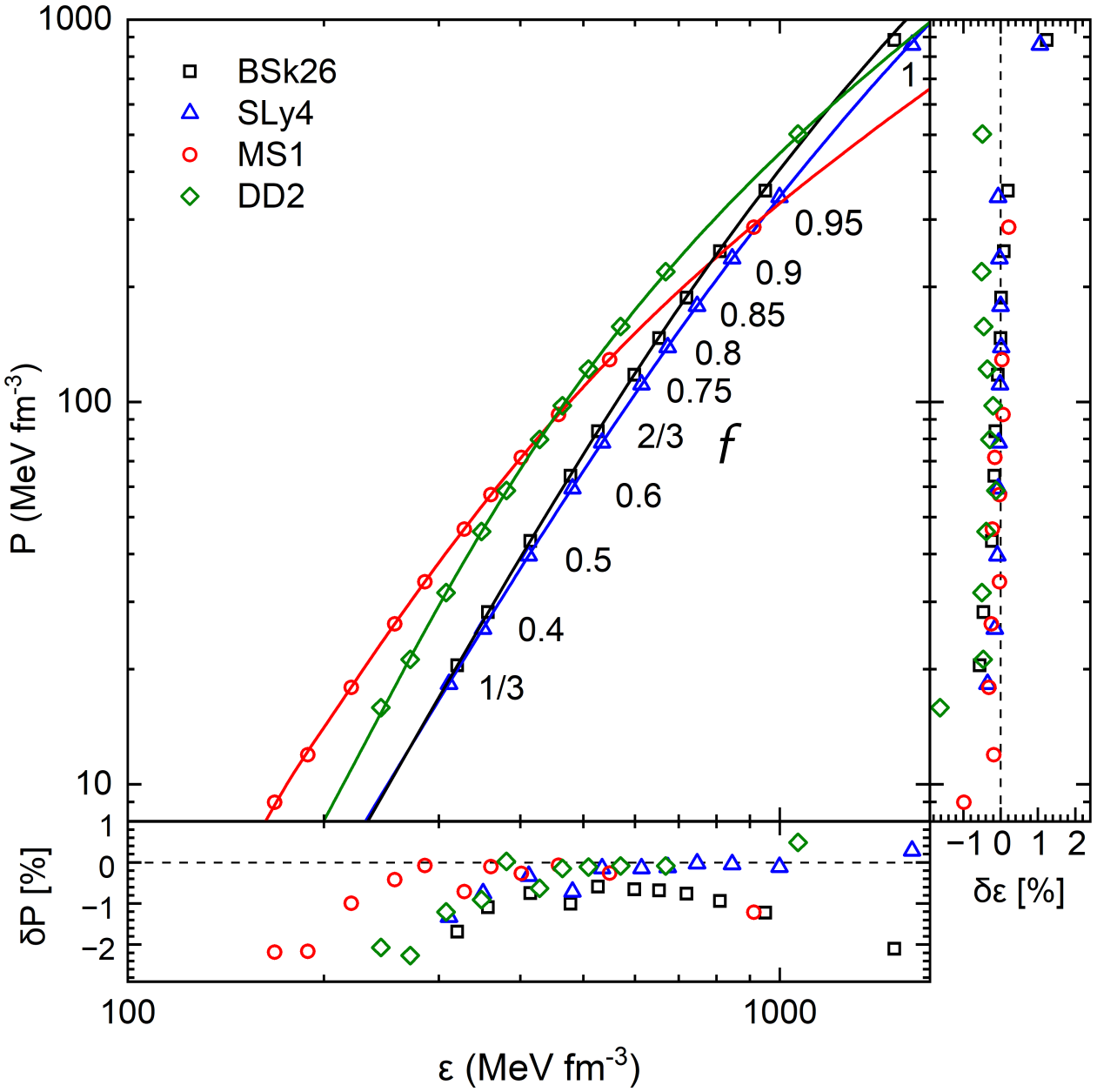

# Testing the Inversion for $c_s^2 - P/\mathcal{E}$

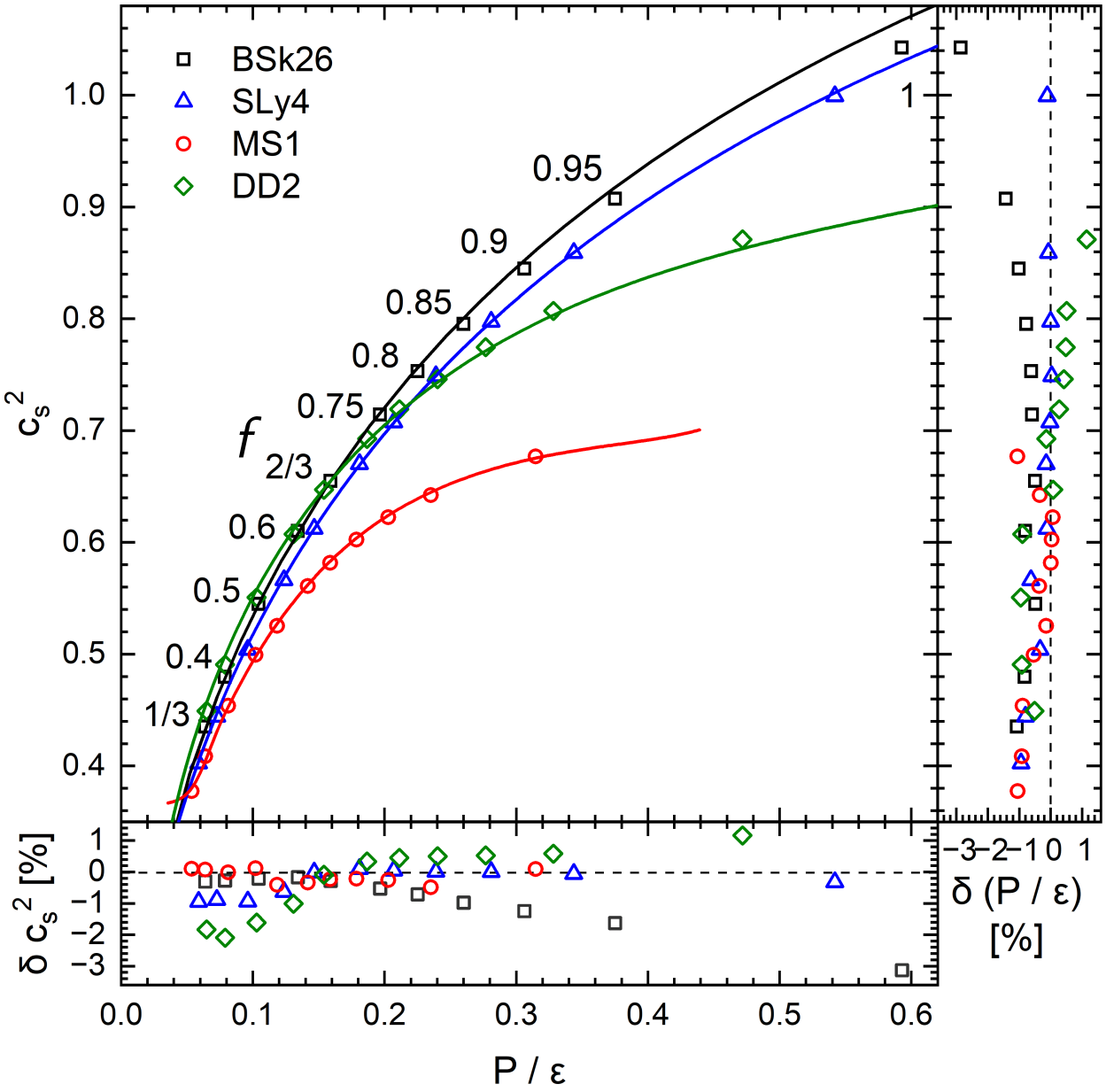

# Inversion of $M - R$ Data

Instead of inverting an $M - R$ curve one may wish to infer the EOS from $M - R$ data. $M_{max}$ and $R_{max}$ are not precisely known. One can form analytical correlations between $(M, R)$ and $(\mathcal{E}_c, P_c)$, but these have only moderate accuracy since this inversion is not unique. More information than the $M - R$ point itself is necessary to improve the inversion.

One possibility is the inverse slope $dR/dM$ at the $(M, R)$ point. Generally, one can express a correlation between a quantity $G = \in [\mathcal{E}_c, P_c, \mathrm{etc.}]$ and $(M, R, dR/dM)$ in the form

$$\ln G = \ln a_G + b_G \ln M + c_G \ln R + d_G (dR/dM).$$

Including $dR/dM$ information improves correlations by factors of about 2. It is also found that inferred values of $\mathcal{E}_c$ and $P_c$ are highly correlated; fits to $P_c/\mathcal{E}_c$ have much smaller uncertainty than fits to $\mathcal{E}_c$ or $P_c$.

One has a few $M - R$ uncertainty regions from observations of different objects. Consider two regions with different average values of $M$. Select random pairs of points from each region; using the above correlation formula, then infer two $\mathcal{E}_c - P_c$ uncertainty regions (after rejecting pairs that violate the conditions $0 \leq dP_c/d\mathcal{E}_c \leq 1$ and $dP_c/dM > 0$).

# Comparison to Traditional Bayesian Inference

Traditional Bayesian inversions begin with an $M - R$ prior generated by sampling millions of trials using a specific EOS parameterization with uniform distributions of parameters within selected ranges.

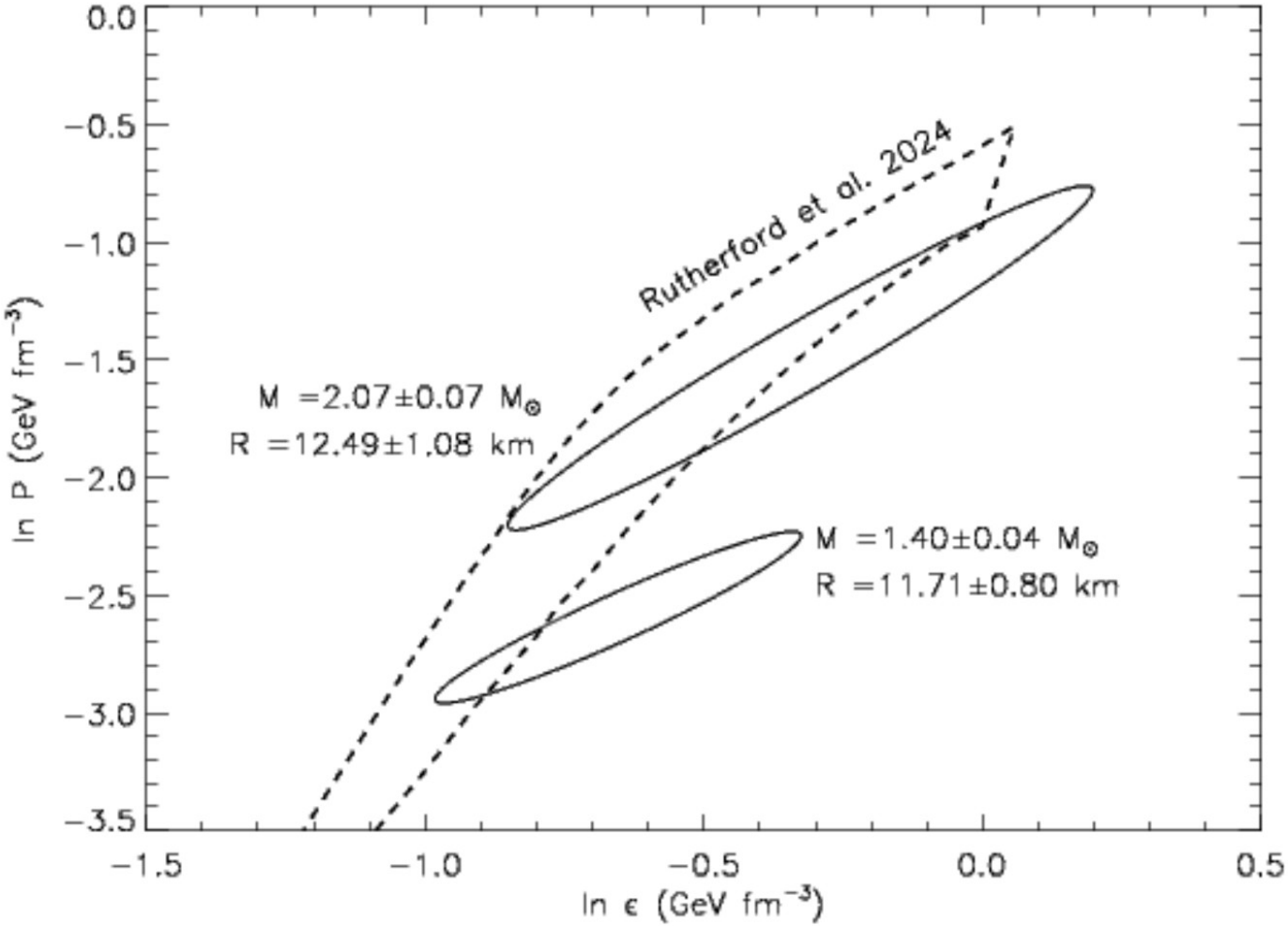

# Importance of $\Delta R = R_{2.0} - R_{1.4}$

- J0437-4715:
$R = 11.36^{+0.95}_{-0.63}$ kn
- J0740+6620:
$R = 12.49^{+1.28}_{-0.88}$ kn

$\Delta R = +1.13^{+1.59}_{-1.08}$ km

313 Skyrme + RMF forces with $M_{max} \geq 2.0 M_\odot$

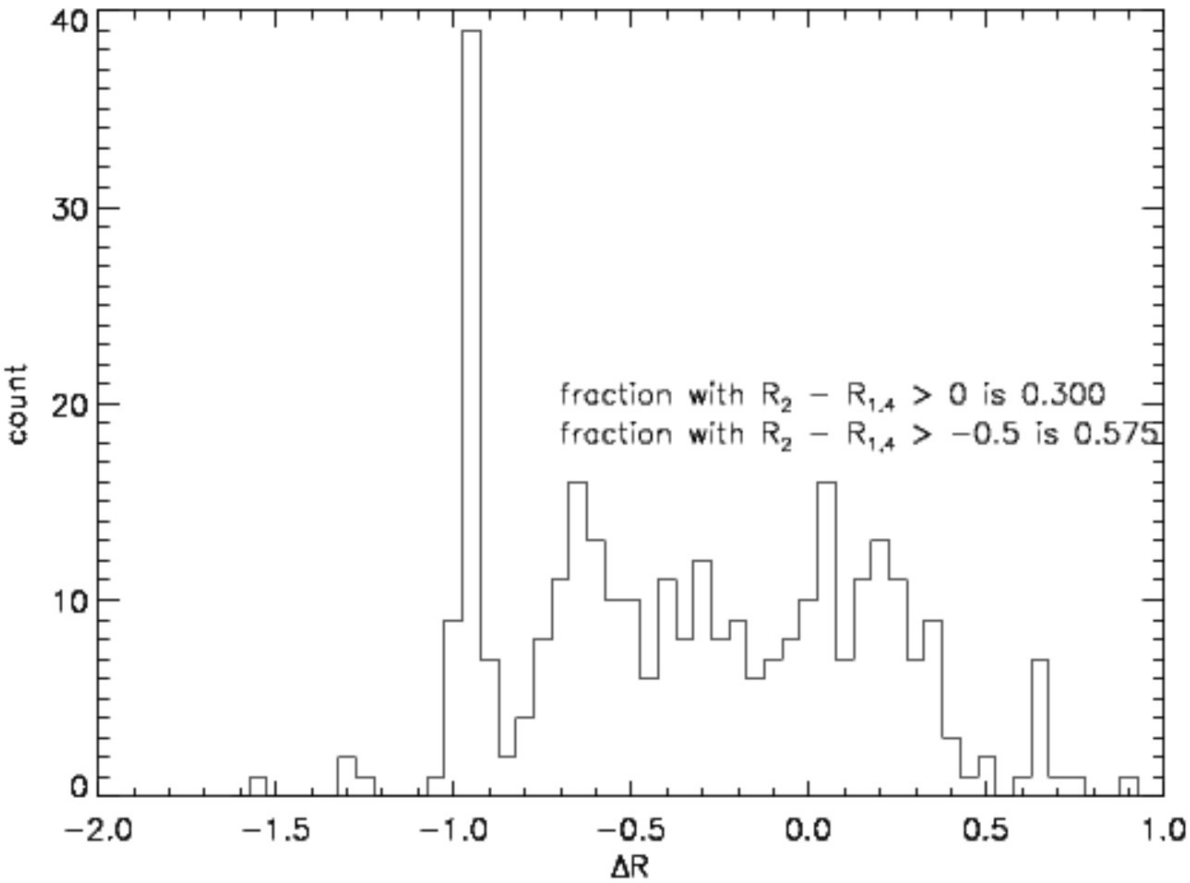

# Applications

- Analytic inversion of TOV equations with arbitrarily high accuracies (depends on number of $R_f$ values).
- Existing techniques use parameterized EOS models in probabilistic (Bayesian) approaches having unquantified systematic uncertainties stemming from the model and parameter choices (prior distributions).

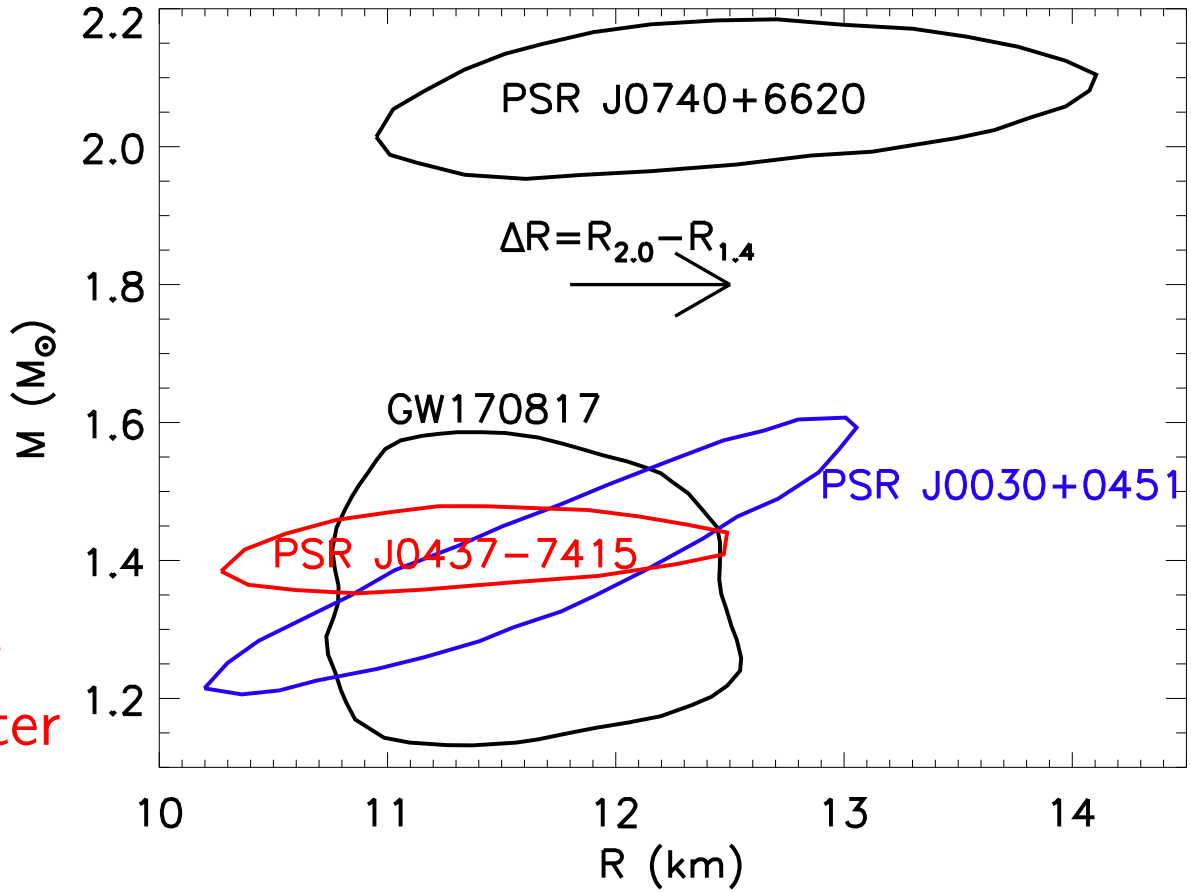

- Since $M$ and $R$ can't uniquely determine $\mathcal{E}_c$ and $P_c$, we use the value of $(dR/dM)$ to improve accuracies.
- Correlations of $c_s$ with $M, R$ and $dR/dM$ can be used to further improve the fidelity of inversions and also for interpolating within the $\mathcal{E}_f - P_f$ grid. They could also allow probing the composition of the neutron star interior (phase transitions, etc.).
- Correlations of $\tilde{\Lambda}, \bar{I}$ and $\mathrm{BE}/M$ with $M$ and $R$ also exist and aren't sensitive to $dR/dM$.